On the Dynamic Characteristics of the Human Skull - Brain System

A. Charalambopoulos, G. Dassios, D.I. Fotiadis,
and C.V. Massalas

7-96

Preprint no. 7-96/1996

Department of Computer Science
University of Ioannina
45 100 Ioannina, Greece

THE DYNAMIC CHARACTERISTICS OF THE HUMAN SKULL - BRAIN SYSTEM

A. CHARALAMBOPOULOS
Institute of Chemical Engineering and High Temperature Chemical Processes, GR 265 00 Patras, Greece

G. DASSIOS
Dept. of Chemical Engineering, University of Patras and Institute of Chemical Engineering and High Temperature Chemical Processes, GR 265 00 Patras, Greece

D.I. FOTIADIS
Dept. of Computer Science, University of Ioannina, GR 451 10 Ioannina Greece

C.V. MASSALAS*
Dept. of Mathematics, University of Ioannina, GR 451 10 Ioannina, Greece

Abstract

In this work the dynamic characteristics of the human skull-brain system is studied. For the purpose of our analysis we adopted a model consisted of a hollow sphere (skull), an inviscid and irrotational fluid (cerebrospinal fluid) and a concentrically located inner elastic sphere (brain). The mathematical analysis is based on the elasticity solution for the elastic spheres and the simplified description of the motion of the fluid by the wave equation. The roots of the characteristic equation were found numerically. The results are in good agreement with other researchers analogous modelling work, however our three dimensional analysis introduces a new pattern of frequencies to the natural frequencies spectra of the skull-brain system. The results are compared with experimental ones and the role of the various system parameters on the natural frequencies is investigated.

1. INTRODUCTION

The knowledge of how and why the natural frequencies change could aid in the development of a new medical instrument for the early diagnosis of brain diseases [1]. The experimental investigations of the resonance frequencies of the human skull have been made on living subjects as well as cadavers and dry skulls. Khalil et al. [2] presented a comprehensive investigation of the resonance frequencies of the human skull. The resonance frequencies of the human skull *in vivo* have been recently investigated by Håkansson et al. [3]. The complexity of the human skull structure presents an extremely difficult task to one wishing to perform detailed simulation of the physical processes of the human head by mathematical modelling. For this reason, geometrical approximations are typically used for analytical investigations. We note that, although finite element model representations of the head geometry are more desirable, compatible characterisations of the zonal scalp, skull, dura matter and brain constitutive properties along with engineering definitions of the associated interface conditions are lacking.

Engin and Liu [4] adopted a model consisting of a thin homogeneous isotropic and spherical shell containing an inviscid irrotational fluid. Advani and Owings [5] considered a structural modelling of the human head consisting of a uniform elastic spherical shell (skull) containing an elastic core (brain). Talhouni and DiMaggio [6] introduced the modelling of a head as a prolate spherical shell filled with an inviscid liquid. The model of Ref. 6 was used by Misra et al. [7] to study the dynamic response of a head-neck system to an impulsive load. Recently, Guarino and Elger [8] adopted the modelling of the human head by a fluid-filled elastic shell containing a concentrically located elastic sphere. In Ref. 8 an analytical modal analysis was used to obtain the characteristic equation for the natural frequencies of the physical system considered. The major assumptions adopted by Guarino and Elger are that the fluid is inviscid, the spherical shell is thin and the modes of the physical system are axisymmetric.

* Author to whom correspondence should be addressed

The effect of viscosity on the free oscillations of fluid-filled spherical shells was studied by Su [9]. From the results cited in Ref. 9 we obtain the information that the natural frequencies of a vibrating spherical shell will decrease with increase of the viscosity of the contained fluid. The elastomechanical characterisation of brain tissues was studied by Sahay et al. [10]. The model used in Ref. 10 consists of an outer shell representing the rigid cranium and an inner sphere representing the hyperelastic brain. The cranium is supposed to be separated from the brain by a bed of venous fluid. A model which takes into account the viscoelastic nature of the brain tissue would be a more accurate representation of the intracranial complex [11].

In this study we adopt a model for the human head consisted of a hollow sphere (skull) containing a concentrically located elastic sphere (brain). The space between the two spheres is supposed to be filled with a fluid (cerebrospinal fluid). The aim of this work is to investigate the dynamic characteristics of the human head. The major assumptions of the system considered are that the fluid is inviscid and irrotational and the skull bones and brain tissue are linear, elastic, isotropic and homogeneous. The analysis is based on the three dimensional theory of elasticity and the representation of the displacement field of the skull and brain in terms of the Navier eigenvectors [12]. The motion of the fluid is supposed to undergo small oscillations governed by the wave equation. The characteristic (frequency) equation of the problem under discussion was solved numerically and results for the eigenfrequencies and mode shapes are presented in tables and graphs. The results obtained are compared with experimental ones. As it is expected the results of Engin and Liu are in better agreement with our results as the shell becomes thinner. The results of Guarino and Elger are in quantitative disagreement with our results and it is supposed to be due to the assumptions introduced in Ref. 8.

From the present analysis we see that the three dimensional analysis predicts an extra pattern of natural frequencies on the frequency spectra of the system considered. We note that the cases of fluid-filled hollow sphere, of three elastic spheres and that of an elastic sphere are also discussed and the role of various parameters on the natural frequencies of the system considered are extensively discussed.

2. PROBLEM FORMULATION

The selected model (Fig. 1) consists of an elastic sphere (2 - skull) containing a concentrically located elastic sphere (0 - brain). The space between the regions 2 and 0 is considered to be filled with a fluid (1 - CSF: cerebrospinal fluid)

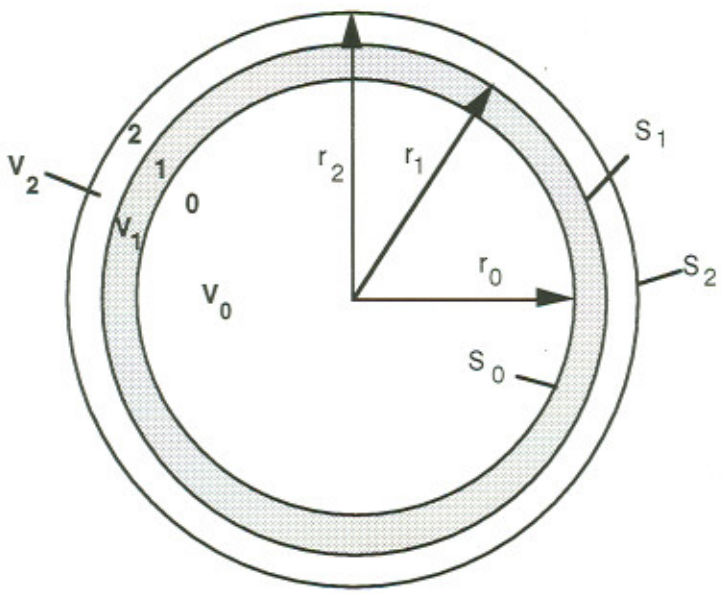

Figure 1: Problem Geometry

The skull bones and brain tissue are assumed to be linear, elastic, isotropic and homogeneous while the fluid is considered inviscid and irrotational. The spherical co-ordinate system is shown in Fig. 2.

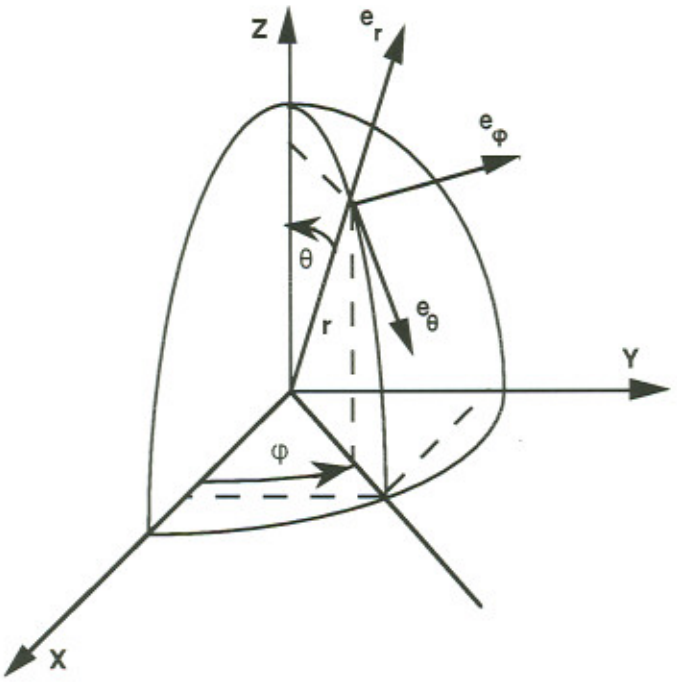

Figure 2: Spherical Polar Coordinate System

For motions in homogeneous isotropic, elastic solids the displacement vector field $\boldsymbol{u} = \boldsymbol{u}(\boldsymbol{r},t)$, satisfies the equation

$$\mu_k \nabla^2 \boldsymbol{u}^{(k)}(\boldsymbol{r},t) + (\lambda_k + \mu_k)\nabla\nabla \cdot \boldsymbol{u}^{(k)}(\boldsymbol{r},t) = \rho_k \frac{\partial^2 \boldsymbol{u}^{(k)}(\boldsymbol{r},t)}{\partial t^2}, \tag{1}$$

where μ_k, λ_k are Lamè's constants, ρ_k is the mass density, ∇ is the usual del operator, t is the time and k=0,2 indicates the brain (k=0) and the skull (k=2), respectively. We note that $\lambda_k + \mu_k = K_k + \frac{\mu_k}{3}$, where K_k is the bulk modulus of the k-medium.

For the free vibration problem we assume that

$$\boldsymbol{u}^{(k)}(\boldsymbol{r},t) = \mathrm{Re}[\boldsymbol{u}_o^{(k)}(\boldsymbol{r})e^{-i\omega t}], \tag{2}$$

where ω denotes the angular frequency measured in radians/sec and $i = \sqrt{-1}$.

Introducing the dimensionless variables

$$\boldsymbol{r}' = \frac{\boldsymbol{r}}{\alpha}, \quad \Omega = \frac{\omega\alpha}{c_{p_2}}, \quad (\alpha = r_2) \tag{3}$$

and (2) into the equation of motion (1) we obtain

$$c'^2_{sk}\nabla'^2 \boldsymbol{u}^{(k)}(\boldsymbol{r}') + (c'^2_{pk} - c'^2_{sk})\nabla'(\nabla' \cdot \boldsymbol{u}_o^{(k)}(\boldsymbol{r}')) + \Omega^2 \boldsymbol{u}_o^{(k)}(\boldsymbol{r}') = 0, \tag{4}$$

where

$$\nabla' = \alpha\nabla, \quad c'_{sk} = \frac{c_{sk}}{c_{p_2}}, \quad c'_{s_k} = \frac{c_{p_k}}{c_{p_2}}, \quad c^2_{s_k} = \frac{\mu_k}{\rho_k}, \quad c^2_{p_k} = \frac{(\lambda_k + 2\mu_k)}{\rho_k}, \quad k = 0,2.$$

The motion of an inviscid and irrotational fluid undergoing small oscillations is governed by the wave equation,

$$\nabla^2\Phi = \frac{1}{c_f^2}\frac{\partial^2\Phi}{\partial t^2}$$

or

$$\nabla'^2\Phi = \frac{1}{c'^2_f}\frac{\partial^2\Phi}{\partial t'^2}\ , \tag{5}$$

where Φ is the velocity potential, c_f is the speed of sound in the fluid and

$$t = \frac{\alpha}{c_{P_2}}t',\quad c'_f = \frac{c_f}{c_{P_2}}\ .$$

Supposing that

$$\Phi(\boldsymbol{r}',t') = \mathrm{Re}[\Phi_o(\boldsymbol{r}')e^{-i\Omega t'}]$$

we obtain

$$\nabla'^2\Phi_o(r') = -k'^2_f\Phi_o(r') \tag{6}$$

where $k'_f = \Omega/c'_f$.

The pressure, P, in the fluid is found from the velocity potential as

$$P = -\rho_f\left(\frac{\partial\Phi}{\partial t}\right), \tag{7}$$

where ρ_f is the mass density of the fluid.

The previous relation in dimensionless form is given as

$$P' = \frac{P}{\mu_2} = i\Omega\rho'_f\frac{1}{c'^2_{s_2}}\Phi_o\ , \tag{8}$$

where $\rho'_f = \rho_f/\rho_2$.

The interaction of the k - media of the system enters the mathematical formulation through the boundary conditions on the surfaces, S_k, $k = 0,1,2$.

We assume that the surface S_2 is stress free, that is

$$\boldsymbol{T}'_2\boldsymbol{u}^{(2)}(\boldsymbol{r}'_2) = \boldsymbol{0} \tag{9}$$

The boundary conditions on $S_k, k = 1,0$ are given as

$$\boldsymbol{T}'_2\boldsymbol{u}^{(2)}(\boldsymbol{r}'_1) = -P'(\boldsymbol{r}'_1)\hat{\boldsymbol{r}} \tag{10a}$$

$$\hat{\boldsymbol{r}}\cdot\boldsymbol{u}^{(2)}(\boldsymbol{r}'_1) = \hat{\boldsymbol{r}}\cdot\boldsymbol{u}^{(1)}(\boldsymbol{r}'_1) \tag{10b}$$

and

$$\boldsymbol{T}'_0 \boldsymbol{u}^{(0)}(\boldsymbol{r}'_0) = -P'(\boldsymbol{r}'_0)\hat{\boldsymbol{r}} \tag{11a}$$

$$\hat{\boldsymbol{r}} \cdot \boldsymbol{u}^{(0)}(\boldsymbol{r}'_0) = \hat{\boldsymbol{r}} \cdot \boldsymbol{u}^{(1)}(\boldsymbol{r}'_0), \tag{11b}$$

respectively,

where

$$T'_i = 2\mu'_i \hat{r} \cdot \nabla' + \lambda'_i \hat{r} \times \nabla' \cdot + \mu'_i \hat{r} \times \nabla, \quad i = 0,2 \tag{12}$$

stands for the dimensionless surface traction operator in V_i, $\hat{\boldsymbol{r}}$ is the unit outward normal vector on S_i and $(\lambda'_i, \mu'_i) = (\lambda_i/\mu_2, \mu_i/\mu_2)$.

From the physical point of view the conditions (10a,11a) say that the radial stress in the regions 2 and 0 at $\boldsymbol{r} = \boldsymbol{r}_1$ and $\boldsymbol{r} = \boldsymbol{r}_o$ is equal and opposite to the fluid pressure at the same surfaces, while (10b, 11b) represent the continuity condition at $S_k, k = 1,0$.

In the course of the present analysis we shall also discuss the cases where
i) the space 1 is filled with an elastic material,
ii) the spaces 0 and 1 are filled with an inviscid and irrotational fluid and
iii) the case of an elastic sphere.

As it is obvious in each case the mathematical problem has to be properly modified. We note that the problem described by the equations of motion (4), (5) and the boundary conditions (9), (10) and (11) is a well - posed mathematical problem.

3. PROBLEM SOLUTION - FREQUENCY EQUATION

In the case of the elastic regions 2 and 0 we represent the displacement field in terms of the Navier eigenvectors [12], that is

$$\boldsymbol{u}_o^{(2)}(\boldsymbol{r}) = \sum_{n=0}^{\infty} \sum_{m=-n}^{n} \sum_{l=1}^{2} \left\{ \alpha_{n,2}^{m,l} \boldsymbol{L}_{n,2}^{m,l}(\boldsymbol{r}) + \beta_{n,2}^{m,l} \boldsymbol{M}_{n,2}^{m,l}(\boldsymbol{r}) + \gamma_{n,2}^{m,l} \boldsymbol{N}_{n,2}^{m,l}(\boldsymbol{r}) \right\}, \quad \boldsymbol{r} \in V_2 \tag{13}$$

and

$$\boldsymbol{u}_o^{(0)}(\boldsymbol{r}) = \sum_{n=0}^{\infty} \sum_{m=-n}^{n} \left\{ \alpha_{n,0}^{m,1} \boldsymbol{L}_{n,0}^{m,1}(\boldsymbol{r}) + \beta_{n,0}^{m,1} \boldsymbol{M}_{n,0}^{m,1}(\boldsymbol{r}) + \gamma_{n,0}^{m,1} \boldsymbol{N}_{n,0}^{m,1}(\boldsymbol{r}) \right\}, \quad \boldsymbol{r} \in V_0 \tag{14}$$

respectively, where

$$\begin{aligned}
\boldsymbol{L}_n^{m,l}(r') &= \dot{g}_n^l(\Omega r') P_n^m(\hat{\boldsymbol{r}}) + \sqrt{n(n+1)} \frac{g_n^l(\Omega r')}{\Omega r'} \boldsymbol{B}_n^m(\hat{\boldsymbol{r}}) \\
\boldsymbol{M}_n^{m,l}(r') &= \sqrt{n(n+1)} g_n^l(k'_s r') \boldsymbol{C}_n^m(\hat{\boldsymbol{r}}) \\
\boldsymbol{N}_n^{m,l}(r') &= n(n+1) \frac{g_n^l(k'_s r')}{k'_s r'} P_n^m(\hat{\boldsymbol{r}}) + \sqrt{n(n+1)} \left\{ \dot{g}_n^l(k'_s r') + \frac{g_n^l(k'_s r')}{k'_s r'} \right\} \boldsymbol{B}_n^m(\hat{\boldsymbol{r}})
\end{aligned} \tag{15}$$

$$k'_{p_i} = \frac{\Omega}{c'_{p_i}} = \begin{cases} \Omega, & i = 2 \\ \Omega / c'_{p_0}, & i = 0 \end{cases}$$

$$k'_{s_i} = \frac{\Omega}{c'_{s_i}} = \begin{cases} \Omega/c'_{s_2}, & i=2 \\ \Omega/c'_{s_0}, & i=0 \end{cases} \tag{16}$$

$$\dot{g}_n^l(z) = \frac{d}{dz}(g_n^l), \quad l=1,2$$

and $g_n^1(z)$ and $g_n^2(z)$ represent the spherical Bessel functions of the first, $j_n(z)$, and second, $y_n(z)$, kind, respectively. The functions $P_n^m(\boldsymbol{r}')$, $B_n^m(\boldsymbol{r}')$ and $C_n^m(\boldsymbol{r}')$ defined on the unit sphere, are the vector spherical harmonics introduced by Hansen and in spherical polar coordinates (r,ϑ,φ) are given as follows

$$\begin{aligned} \boldsymbol{P}_n^m(\hat{r}) &= \hat{r}Y_n^m(\hat{r}) \\ \boldsymbol{B}_n^m(\hat{r}) &= \frac{1}{\sqrt{n(n+1)}}\left\{\hat{\vartheta}\frac{\partial}{\partial\vartheta} + \hat{\varphi}\frac{1}{\sin\vartheta}\frac{\partial}{\partial\varphi}\right\}Y_n^m(\hat{r}) \\ \boldsymbol{C}_n^m(\hat{r}) &= \frac{1}{\sqrt{n(n+1)}}\left\{\hat{\vartheta}\frac{1}{\sin\vartheta}\frac{\partial}{\partial\varphi} - \hat{\varphi}\frac{\partial}{\partial\vartheta}\right\}Y_n^m(\hat{r}), \end{aligned} \tag{17}$$

where $\hat{\vartheta}$ and $\hat{\varphi}$ are the unit vectors in ϑ and φ - directions, respectively, $Y_n^m(\hat{r}) = P_n^m(\cos\vartheta)e^{im\varphi}$ are the spherical harmonics and $P_n^m(\cos\vartheta)$ are the well known Legendre functions.

The spherical polar coordinates of the real part of the displacement field as well as the expressions $\boldsymbol{T}'_i\boldsymbol{L}_n^{m,l}(\hat{\boldsymbol{r}}')$, $\boldsymbol{T}'_i\boldsymbol{M}_n^{m,l}(\hat{\boldsymbol{r}}')$ and $\boldsymbol{T}'_i\boldsymbol{N}_n^{m,l}(\hat{\boldsymbol{r}}')$ are given in Appendix A.

In the case of fluid the velocity potential Φ is given as

$$\Phi_o(r') = \sum_{n=0}^{\infty}\sum_{m=-n}^{n}\left\{c_{m,n}g_n^1(k'_f r') + \varepsilon d_{m,n}g_n^2(k'_f r')\right\}P_n^m(\cos\vartheta)e^{im\varphi} \tag{18}$$

where

$$\varepsilon = \begin{cases} 1, & r_0 \neq 0 \\ 0, & r_0 = 0 \end{cases}.$$

The velocity of the fluid is expressed as

$$\boldsymbol{T}'\boldsymbol{v}'(\boldsymbol{r}',t') = \nabla'\Phi = k'_f\sum_{n=0}^{\infty}\sum_{m=-n}^{n}\left\{\begin{aligned}&\left[c_{nm}\dot{g}_n^1(k'_f r') + \varepsilon d_{nm}\dot{g}_n^2(k'_f r')\right]\boldsymbol{P}_n^m(\hat{\boldsymbol{r}}) \\ &+\left[c_{nm}g_n^1(k'_f r') + \varepsilon d_{nm}g_n^2(k'_f r')\right]\frac{1}{r'}\sqrt{n(n+1)}\boldsymbol{B}_n^m(\hat{\boldsymbol{r}})\end{aligned}\right\}e^{-i\Omega t'}\boldsymbol{N}_n^{m,l}(\hat{\boldsymbol{r}}')$$

and the corresponding displacement field is

$$\boldsymbol{u}^{(1)}(\boldsymbol{r}',t') = \frac{i}{\Omega}\boldsymbol{v}(\boldsymbol{r}') = \frac{i}{c'_f}\sum_{n=0}^{\infty}\sum_{m=-n}^{n}\left\{\begin{aligned}&\left[c_{nm}\dot{g}_n^1(k'_f r') + \varepsilon d_{nm}\dot{g}_n^2(k'_f r')\right]\boldsymbol{P}_n^m(\hat{\boldsymbol{r}}) \\ &+\left[c_{nm}g_n^1(k'_f r') + \varepsilon d_{nm}g_n^2(k'_f r')\right]\frac{1}{r'}\sqrt{n(n+1)}\boldsymbol{B}_n^m(\hat{\boldsymbol{r}})\end{aligned}\right\}e^{-i\Omega t'}. \tag{19}$$

The expression for the pressure is found by replacing the expression (18) for the velocity potential Φ into (8), that is

$$P' = i\Omega\rho'_f \frac{1}{c'^2_{s_2}}\Phi = i\Omega\rho'_f \frac{1}{c'^2_{s_2}}\sum_{n=0}^{\infty}\sum_{m=-n}^{n}\left\{c_{m,n}g_n^1(k'_f r') + \varepsilon d_{m,n}g_n^2(k'_f r')\right\}P_n^m(\cos\vartheta)e^{im\varphi}. \quad (20)$$

Since the expressions (13), (14) and (18) satisfy the equations (1) and (5), respectively, it remains to ask the boundary conditions (9), (11) and (12) to be satisfied.

The application of the boundary conditions (for the case $r'_0 \neq 0$) give

At $r = r_2$:

$$\boldsymbol{T}'_2 \boldsymbol{u}^{(2)}(\boldsymbol{r}'_2) = 0$$

or

$$\sum_{l=1}^{2}\left[\alpha_{n,2}^{m,l}A_{n,2}^l(r'_2) + \gamma_{n,2}^{m,l}D_{n,2}^l(r'_2)\right] = 0 \quad (21a)$$

$$\sum_{l=1}^{2}\left[\alpha_{n,2}^{m,l}B_{n,2}^l(r'_2) + \gamma_{n,2}^{m,l}E_{n,2}^l(r'_2)\right] = 0 \quad (21b)$$

$$\sum_{l=1}^{2}\beta_{n,2}^{m,l}\Gamma_{n,2}^l(r'_2) = 0. \quad (21c)$$

At $r = r_1$:

$$\boldsymbol{T}'_2 \boldsymbol{u}^{(2)}(\boldsymbol{r}'_1) = -P'(\boldsymbol{r}'_1)\hat{\boldsymbol{r}}$$

or

$$\sum_{l=1}^{2}\left[\alpha_{n,2}^{m,l}A_{n,2}^l(r'_2) + \gamma_{n,2}^{m,l}D_{n,2}^l(r'_2)\right] = -i\Omega\rho'_f \frac{1}{c'^2_{s_2}}\left[c_{nm}g_n^1(k'_f r'_1) + d_{nm}g_n^2(k'_f r'_1)\right] \quad (22a)$$

$$\sum_{l=1}^{2}\left[\alpha_{n,2}^{m,l}B_{n,2}^l(r'_1) + \gamma_{n,2}^{m,l}E_{n,2}^l(r'_1)\right] = 0 \quad (22b)$$

$$\sum_{l=1}^{2}\beta_{n,2}^{m,l}\Gamma_{n,2}^l(r'_1) = 0 \quad (22c)$$

and

$$\hat{\boldsymbol{r}}\cdot\boldsymbol{u}^{(2)}(\boldsymbol{r}'_1) = \hat{\boldsymbol{r}}\cdot\boldsymbol{u}^{(1)}(\boldsymbol{r}'_1):$$

or

$$\sum_{l=1}^{2}\left[\alpha_{n,2}^{m,l}\dot{g}_n^l(\Omega r'_1)+\gamma_{n,2}^{m,l}n(n+1)\frac{g_n^l(k'_{s_2}r'_1)}{k'_{s_2}r'_1}\right]= \frac{i}{c'_f}\left[c_{nm}\dot{g}_n^1(k'_f r'_1)+d_{nm}\dot{g}_n^2(k'_f r'_1)\right] \tag{23}$$

At $r=r_0$:

$$\boldsymbol{T}'_0\boldsymbol{u}^{(0)}(\boldsymbol{r}'_0)=-P'(\boldsymbol{r}'_0)\hat{\boldsymbol{r}}$$

or

$$\alpha_{n,0}^{m,l}A_{n,0}^l(r'_0)+\gamma_{n,0}^{m,l}D_{n,0}^l(r'_0)= -i\Omega\rho'_f\frac{1}{c'^2_{s_2}}\left[c_{nm}g_n^1(k'_f r'_0)+d_{nm}g_n^2(k'_f r'_0)\right] \tag{24a}$$

$$\alpha_{n,0}^{m,l}B_{n,0}^l(r'_0)+\gamma_{n,0}^{m,l}E_{n,0}^l(r'_0)=0 \tag{24b}$$

$$\beta_{n,0}^{m,l}\Gamma_{n,0}^l(r'_0)=0 \tag{24c}$$

and

$$\hat{\boldsymbol{r}}\cdot\boldsymbol{u}^{(1)}(\boldsymbol{r}'_0)=\hat{\boldsymbol{r}}\cdot\boldsymbol{u}^{(0)}(\boldsymbol{r}'_0)$$

or

$$\alpha_{n,0}^{m,l}\dot{g}_n^l(\Omega r'_0)+\gamma_{n,0}^{m,l}n(n+1)\frac{g_n^l(k'_{s_2}r'_0)}{k'_{s_2}r'_0}= \frac{i}{c'_f}\left[c_{nm}\dot{g}_n^1(k'_f r'_0)+d_{nm}\dot{g}_n^2(k'_f r'_0)\right] \tag{25}$$

where

$$A_{n,i}^l(r')=-\left[\frac{4\mu'_i}{r'}\dot{g}_n^l(k'_{pi}r')+2\mu_i k'_{pi}\left(1-\frac{n(n+1)}{k'^2_{pi}r'^2}\right)g_n^l(k'_{pi}r')+\lambda'_i k'_{pi}\dot{g}_n^l(k'_{pi}r')\right]$$

$$B_{n,i}^l(r')=2\mu'_i\sqrt{n(n+1)}\left[\frac{1}{r'}\dot{g}_n^l(k'_{pi}r')-\frac{g_n^l(k'_{pi}r')}{k'_{pi}r'^2}\right]$$

$$\Gamma_{n,i}^l(r')=\mu'_i\sqrt{n(n+1)}\left[k'_{si}\dot{g}_n^l(k'_{si}r')-\frac{1}{r'}g_n^l(k'_{si}r')\right]$$

$$D_{n,i}^l(r')=2\mu'_i n(n+1)\left[\frac{\dot{g}_n^l(k'_{si}r')}{r'}-\frac{g_n^l(k'_{si}r')}{k'_{si}r'^2}\right]$$

$$E^{l}_{n,i}(r') = \mu'_i \sqrt{n(n+1)} \left[-2\frac{\dot{g}^{l}_{n}(k'_{si} r')}{r'} - k'_{si}\, g^{l}_{n}(k'_{si} r') + 2\frac{n(n+1)-1}{k'_{si} r'^{2}} g^{l}_{n}(k'_{si} r') \right].$$

The system of the algebraic equations (21) - (25) can be written as

$$\boldsymbol{D}\boldsymbol{x} = \boldsymbol{0}. \tag{26}$$

Details about the system (26), for each case under discussion, are given in Appendix B.

In order for the system (26) to have a non-trivial solution, the following condition has to be satisfied

$$\det(\boldsymbol{D}) = 0. \tag{27}$$

This condition provides the characteristic (frequency) equation, the roots of which are the eigenfrequency coefficients Ω of the system under discussion. The mode shape corresponding to each Ω is obtained by solving the system (26).

4. NUMERICAL RESULTS - DISCUSSION

The frequency equation (27) has been solved numerically and for this purpose a matrix determinant computation routine was used for different frequency coefficients Ω, along with a bisection method to refine steps close to its roots. The root finding algorithm is followed by an LU - decomposition and back-substitution routine to determine the eigenvectors, whose elements are used for the computation of the corresponding displacement components.

The main purpose of our analysis is the modelling of the cranial system. The system is composed from the skull bones, the cerebrospinal fluid and the brain. In the present analysis we assume that the properties of the cranial components are:

Skull [13]

$$E = 6.5x10^{9}\, N/m^{2},\quad \nu = 0.25,\quad \rho = 2.1326x10^{3}\, Kg/m^{3},$$

Cerebrospinal Fluid (CSF)[14]

$$K = 2.1029753x10^{9}\, N/m^{2},\quad \rho = 1.0002x10^{3}\, Kg/m^{3},$$

Brain [15]

Fluid: $K = 2.102975x10^{9}\, N/m^{2},\quad \rho = 1.007x10^{3}\, Kg/m^{3}$

Elastic: $E = 2.52357x10^{8}\, N/m^{2},\quad \nu = 0.48,\quad \rho = 1.007x10^{3}\, Kg/m^{3},$

where E, K and ν denote the Young modulus, bulk modulus and Poisson ratio, respectively. The elastic material constants are related as $\mu = \dfrac{E}{2(1+\nu)}$ and $\lambda = \dfrac{E\nu}{(1+\nu)(1-2\nu)}$,

and the geometry of the system is defined by

$$r_2 = 0.082 \text{ m},\quad r_1 = 0.076 \text{ m},\quad r_0 = 0.070 \text{ m}.$$

In Ref. 12 the authors of the present work presented the dynamic characteristics of the human skull which are in good agreement with the existing experimental ones. For the purpose of comparison, in Table 1 the reproduced frequency coefficients of Ref. 4 are shown, as well as those obtained by the present analysis. As it is expected, the results of Engin and Liu are in better agreement with our results (three dimensional theory of elasticity), as the shell becomes thinner. In the case of an elastic spherical shell in vacuo (skull) we observe that for h/R=20 the difference between the compared results is about 3.1 % while for h/R=10 the difference becomes 7.5 %.

Table 1: Eigenfrequency Coefficiecients $\overline{\Omega}_n = \omega\,\alpha/c_f$ of Engin and Liu [4]

Fluid Filled Shell (v=0.3, f=9.38, s=0.553, h/R=1/20)														
No	n=0		n=1		n=2		n=3		n=4		n=5		n=6	
	Engin & Liu	Present Analysis	Engin & Liu	Present Analysis	Engin & Liu	Present Analysis	Engin & Liu	Present Analysis	Engin & Liu	Present Analysis	Engin & Liu	Present Analysis	Engin & Liu	Present Analysis
1	3.1025	3,0901	2.0658	1.9888	0.6042	0.5984	0.7875	0.7780	0.9285	0.9144	1.0684	1.0477	1.2311	1.1856
2	5.8159	5.8046	4.3021	4.2874	4.0321	2.0861	5.7451	3.2985	7.1763	4.4254	8.372	5.5194	9.5119	6.5969
3	8.6877	8.6735	7.1255	7.1138	5.4983	3.8918	6.7777	5.5681	8.2782	7.0218	9.9656	8.2648	11.7123	9.4014
4	11.6535	11.6342	10.0745	10.0584	8.3902	5.4761	9.6252	6.7221	10.8399	8.1276	12.0417	9.7052	13.2210	11.3557
5	14.6756	14.6502	13.0888	13.0668	11.4167	8.3779	12.7261	9.6132	14.0099	10.8287	15.2734	12.0332	16.5110	13.2360
6	17.7321	17.7004	16.1419	16.1135	14.4820	11.3984	15.8424	12.7054	17.1765	13.9869	18.4890	15.2482	19.7110	16.4933
7	20.8108	20.7725	19.2194	19.1842	17.5693	14.4569	18.9654	15.8141	20.3355	17.4448	21.6830	18.4537	23.0010	19.7442
8	23.9044	23.8592	22.3127	22.2707	20.6707	17.5374	22.0926	18.9298	23.4894	20.2959	24.8649	21.6403	26.2110	22.9656
9	27.0081	26.9560	25.4168	25.3679	23.7816	20.6319	25.2227	22.0499	26.6402	23.4427	28.0371	24.8139	29.4010	26.1665
10	30.1192	30.0601	28.5285	28.4728	26.8989	23.7358	28.3552	25.1731	29.7889	26.5864	31.2029	27.9788	32.5810	29.3529
Skull in vacuo (v=0.3, f=0, s=0.553, h/R=1/20)														
No	n=0		n=1		n=2		n=3		n=4		n=5		n=6	
	Engin & Liu	Present Analysis	Engin & Liu	Present Analysis	Engin & Liu	Present Analysis	Engin & Liu	Present Analysis	Engin & Liu	Present Analysis	Engin & Liu	Present Analysis	Engin & Liu	Present Analysis
1	2.9159	2.8428	3.5716	3.4789	1.2707	1.2382	1.5208	1.4796	1.6560	1.6067	1.7871	1.7260	1.9557	1.8766
2						2.0845		3.2959		4.4219		5.5151		6.5917
3					4.9238	4.9727	6.5758	6.3986	8.3155	8.0897	10.0866	9.8106	11.8718	11.5442
Skull in vacuo (v=0.3, f=0, s=0.553, h/R=1/10)														
1	2.9159	2.7770	3.5727	3.3907	1.2801	1.2151	1.5788	1.4882	1.8331	1.7023	2.1738	1.9760	2.6438	2.3437
2						2.0320		3.2129		4.3105		5.3760		6.4255
3					4.9291	4.6648	6.5850	6.2243	8.3282	7.8651	10.1027	9.5324	11.8914	11.2087

Table 2: Eigenfrequency Coefficients of Guarino and Elger [8]

	Fluid Filled Rigid shell		Fuid filled elastic shell with 2 cm rigid sphere		Fluid filled elastic shell with 1cm elastic sphere		Elastic shell in vacuo		Fluid filled elastic shell		Fluid filled elastic shell with 2cm stiff sphere		Fluid filled elastic shell with 2cm elastic sphere	
n	Guarino and Elger	Present Analysis	Guarino and Elger	Present Analysis	Guarino and Elger	Present Analysis	Guarino and Elger	Present Analysis	Guarino and Elger	Present Analysis	Guarino and Elger	Present Analysis	Guarino and Elger	Present Analysis
0	4.4899 7.7191	4.7272 8.1272	3.1553 5.9825 9.5852	3.2771 6.2701 10.1360	3.0616 5.5096 8.3877	3.1713 4.2364 5.7244 7.3654 8.7571	2.8637	2.8668	3.0589 5.4925 8.3317	3.1682 5.7044 8.6918	3.1272 5.8486 9.2549	3.2454 6.1145 9.7467	 3.0780 5.5904 8.5486	2.1182 3.1898 3.6827 5.1340 5.8160 6.5444 7.9352 8.9300
1	2.0858 5.4971 9.2156	3.0508 6.4979 9.8434	1.7750 4.1510 6.9389	2.0253 4.3031 7.2415	1.7743 4.1317 6.6096 6.7636 9.7285	2.0253 4.2851 6.6113 7.0393 9.9304	3.424	3.5000	1.7744 4.1324 6.7628 9.7275	2.0254 4.2852 7.0402 10.1584	1.7748 4.1455 6.8914	2.0251 4.2962 7.1813	1.7737 3.3060 4.1315 6.3977 6.7908 9.2166 9.8687	2.0247 3.3060 4.2851 4.9652 6.3990 7.0747 7.8353 9.2190 10.3273
2	3.3184 7.2625	3.5035 7.6568	0.7157 3.8147 5.2492 7.8267	0.8261 2.2145 3.8844 5.4348 8.1412	0.7162 3.6252 3.8226 5.2840 8.0125 9.2494	0.8267 2.2145 3.6255 3.8930 4.3094 5.4774 8.3531 9.2514	1.1738 4.7695	1.3163 2.1445 4.8520	0.7162 3.8208 5.2829 8.0111	0.8267 2.2145 3.8914 5.4762 8.3525	0.7157 3.8134 5.2331 7.5044 9.6624	0.8261 2.2145 3.8829 5.4126 7.7142 9.9328	0.7156 1.8141 3.8217 4.6234 5.2897 7.6247 8.0303	0.8259 1.8142 2.1547 3.8923 4.6240 5.4833 6.1476 7.6255 8.3742 9.0583
3	4.4882 8.5593	4.7340 9.0188	0.9921 5.4284 6.5789 9.1762	1.0434 3.5014 5.4968 6.7983 9.5171	0.9921 5.2165 5.4332 6.5881 9.2389	1.0794 3.5014 5.4411 6.6588 9.6435	1.5270 6.4011	1.6064 3.5014 6.5093	0.9921 5.4328 6.5880 9.2387	1.0794 3.5013 5.5001 6.8077 9.6432	0.9921 5.4276 6.5762 9.1002	1.0794 3.5014 5.4962 6.7953 9.4039	0.9921 2.6086 5.4317 5.8860 6.5918 8.8105 9.2489	1.0793 2.7213 3.3294 3.5014 5.4990 5.8865 6.8110 7.2753 8.8142 9.6616
4	5.6201 9.8184	5.7321 10.1416	1.2638 6.7827 8.2158	1.3265 4.6975 6.8721 8.3305	1.2638 6.7837 7.0738 8.2167	1.3146 4.6975 6.8732 7.0735 8.3323	1.8319 8.2231	1.8410 4.6975 8.2483	1.2638 6.7837 8.2167	1.3146 4.6974 6.8732 8.3322	1.2638 6.7825 8.2156	1.3146 4.6975 6.8719 8.3301	1.2638 6.7827 7.0918 8.2171 9.9800	1.3146 3.5367 4.3890 4.6975 6.8716 7.0924 8.3329 9.9819

From the results obtained we see that for n≥2 the three dimensional theory predicts an extra pattern of natural frequencies on the frequency spectra of the system considered (fluid - filled and in vacuo elastic sphere).

The fluid - filled elastic shell containing an elastic sphere was studied in Ref. 8 where extensive results for the natural frequencies are cited. The results of Ref. 8 as well as those using the present analysis are presented in Table 2, with material constants [8]:

$$E_2 = 1.38x10^{10}\ N/m^2, \nu_2 = 0.25, \rho_2 = 2132.6\,Kg/m^3, r_2 = 0.08001m$$
$$c_1 = 1450\,m/s, \rho_1 = 1000\,Kg/m^3, r_1 = 0.07239m$$
$$E_0 = 3.4x10^8\ N/m^2, \nu_0 = 0.478, \rho_0 = 1070\,Kg/m^3\ (elastic\ \ sphere)$$
$$E_0 = 1x10^{10}\ N/m^2, \nu_0 = 0.25, \rho_0 = 1000\,Kg/m^3\ (stiff\ \ sphere).$$

From the results comparison one can lead to the conclusion that there is a great quantitative disagreement between our results and those of Ref. 8 even in the case of skull in vacuo, where the present results are in excellent agreement with the previous ones existing in the literature [2]. The reason of the disagreement observed, perhaps, is due to the assumptions adopted by Guarino and Elger.

In Table 3 the first ten eigenfrequency coefficients, $\Omega^{(k)}, k = 1,2,....,10$, are cited for the models considered (skull - S, fluid - filled skull - FF, fluid-filled skull with an elastic core - FFE, three elastic spheres - EEE, and elastic sphere - E) by using the present analysis. We observe that for the k-th eigenfrequency of each model we have the arrangement

$$\Omega^{(k)}(FFE) < \Omega^{(k)}(FF) < \Omega^{(k)}(EEE) < \Omega^{(k)}(S) < \Omega^{(k)}(E)$$

where $k = 1,2,...,8$. This arrangement for $k > 8$ ceases to exist.

Table 3: Comparison of $\Omega^{(k)}, k = 1,2,....,10$

	Fluid Filled with an Elastic Core (FFE)	Fluid Filled Skull (FF)	Three Elastic Spheres (EEE)	Skull (S)	Elastic Sphere (E)
1	0.2109 (n=2)	0.4082 (n=2)	0.5709 (n=2)	0.7083 (n=2)	1.0038 (n=0)
2	0.3252 (n=3)	0.5285 (n=3)	0.7308 (n=1)	0.8522 (n=3)	1.0211 (n=2)
3	0.4378 (n=4)	0.6291 (n=4)	0.8709 (n=2)	0.9486 (n=4)	1.0847 (n=2)
4	0.5649 (n=5)	0.7437 (n=5)	0.9653 (n=3)	1.0631 (n=5)	1.5174 (n=1)
5	0.7006 (n=6)	0.8886 (n=6)	1.0577 (n=2)	1.1971 (n=2)	1.5778 (n=3)
6	0.9029 (n=2)	1.0601 (n=7)	1.2409 (n=3)	1.2184 (n=6)	1.6220 (n=3)
7	0.9514 (n=1)	1.1971 (n=2)	1.3019 (n=4)	1.4210 (n=7)	1.7452 (n=0)
8	0.9677 (n=2)	1.2092 (n=1)	1.3209 (n=0)	1.5479 (n=1)	2.0799 (n=4)
9	1.1065 (n=7)	1.3405 (n=8)	1.3279 (n=1)	1.6695 (n=8)	2.1481 (n=2)
10	1.1971 (n=2)	1.8928 (n=3)	1.5505 (n=4)	1.8928 (n=3)	2.3529 (n=1)

As it is obvious the eigenfrequencies of the system depend on the geometry of the system as well as on its physical properties. For the FF - model we parametrized the first eigenfrequency coefficients Ω_n as

$$\min \Omega_n = \min \overline{\Omega}_n(\nu, \frac{\rho_1}{\rho_2}, \frac{r_2 - r_1}{r_2}), \quad n = 0,1,...,4$$

and the results are cited in Table 4. We observe that as $\frac{\rho_1}{\rho_2}$ is decreasing $\min \Omega_n$ is increasing and as ν is increasing $\min \Omega_n$ is decreasing (for the same n).

Table 4: FF - model : Parametrization of $\min \Omega_n$, $n = 0,1,...,4$

variation of $\frac{r_2 - r_1}{r_2}$					
$\frac{r_2 - r_1}{r_2}$	n=0	n=1	n=2	n=3	n=4
Thin Shell	5.2579	1.0544	1.1548	1.8259	2.4496
0.146	4.3272	1.3516	0.5497	0.7362	0.9470
0.268	3.6429	1.5724	0.7278	1.0725	1.5076
0.390	3.1801	1.7726	0.9014	1.4277	2.0044
0.634	2.7043	1.9955	1.2736	2.0755	2.8057
0.817	2.5827	1.9868	1.4436	2.2312	2.8912
Elastic Sphere	2.5634	1.9772	1.4440	2.2313	2.8921
variation of $\frac{\rho_1}{\rho_2}$					
$\frac{\rho_1}{\rho_2}$	n=0	n=1	n=2	n=3	n=4
1.407	3.1327	1.1104	0.2663	0.3534	0.4316
1.0	3.6265	1.1329	0.3074	0.4053	0.4918
0.703	4.1736	1.1634	0.3531	0.4619	0.5558
0.469	4.8187	1.2092	0.4083	0.5285	0.6291
0.234	7.1520	1.7401	0.6760	0.8204	0.9199
variation of ν					
v	n=0	n=1	n=2	n=3	n=4
0.20	4.9898	1.2241	0.4277	0.5517	0.6551
0.25	4.8187	1.2092	0.4083	0.5285	0.6291
0.30	4.5690	1.1737	0.3825	0.4970	0.5932
0.40	3.6584	0.9881	0.2985	0.3909	0.4695
0.48	1.8258	0.5150	0.1457	0.1920	0.2321

For the model (FFE) we studied the parametrization

$$\min \Omega_n = \min \overline{\Omega}_n(\nu_2, \nu_0, \frac{r_2 - r_1}{r_2}, \frac{r_0}{r_2}), \quad n = 0,1,...,4$$

and the results are presented in Table 5. It is observed that the effect of $\nu_i, i = 0,2$ on $\min \Omega_n$ is analogous to that we discussed for the (FF) model, while the effect of increment of $\frac{r_2 - r_1}{r_2}$ or $\frac{r_0}{r_2}$ is increment of $\min \Omega_n$, n=0,1,..,4 (for same n).

Table 5: FFE - model: parametrization of $\min \Omega_n$, $n = 0,1,\ldots,4$

variation of $\frac{r_0}{r_2}$					
$\frac{r_0}{r_2}$	n=0	n=1	n=2	n=3	n=4
No Fluid	0.8764	1.2073	0.8782	1.2573	1.5676
0.854	0.9514	1.2079	0.2109	0.3252	0.4378
0.732	1.1099	1.2083	0.3232	0.4648	0.5859
0.610	1.3319	1.2085	0.3758	0.5116	0.6212
0.366	2.2199	1.2088	0.4060	0.5281	0.6291
0.183	4.4398	1.2088	0.4082	0.5285	0.6291
Fluid Filled Elastic Sphere	4.8187	1.2092	0.4083	0.5285	0.6291
variation of ν_2					
ν_2	n=0	n=1	n=2	n=3	n=4
0.20	0.9887	1.2228	0.2204	0.3390	0.4556
0.25	0.9514	1.2079	0.2109	0.3252	0.4378
0.30	0.8982	1.1724	0.1980	0.3061	0.4130
0.40	0.7119	0.9866	0.1553	0.2413	0.3272
0.48	0.3516	0.5139	0.0761	0.1188	0.1538
variation of ν_0					
ν_0	n=0	n=1	n=2	n=3	n=4
0.20	4.0920	1.2080	0.2266	0.3406	0.4525
0.25	3.6600	1.2080	0.2264	0.3404	0.4523
0.30	3.2101	1.2080	0.2260	0.3400	0.4520
0.40	2.1873	1.2080	0.2243	0.3384	0.4504
0.48	0.9514	1.2079	0.2109	0.3252	0.4378
variation of $\frac{r_2 - r_1}{r_2}$					
$\frac{r_2 - r_1}{r_2}$	n=0	n=1	n=2	n=3	n=4
0.073	0.9514	1.2079	0.2109	0.3252	0.4378
0.146	1.0406	1.3494	0.3126	0.5017	0.7220
0.268	1.2043	1.5695	0.4323	0.7503	1.1438
0.390	1.4446	1.7701	0.5780	1.0306	1.5489
0.634	2.4129	1.9949	1.0528	1.8527	2.6809

In Figure 3 are shown the frequency spectra for the models considered in the present study. From these results one can see the influence of the cerebrospinal fluid and the brain on the natural frequencies of the human skull. The inner elastic sphere (brain) introduces a pattern of additional frequencies to the spectra of eigenfrequencies of the physical system. The same happens with the EEE - model.

Mode shapes for selected eigenfrequencies are presented in Fig. 4. The total mode of the physical system corresponding to Ω_n is the superposition of the displacements components $(u_r, u_\varphi, u_\vartheta)$. The general shapes of $u_r, u_\varphi, u_\vartheta$ depend upon the order of n while the relative amplitudes of them corresponding to a particular frequency Ω_n depend upon the value of Ω_n.

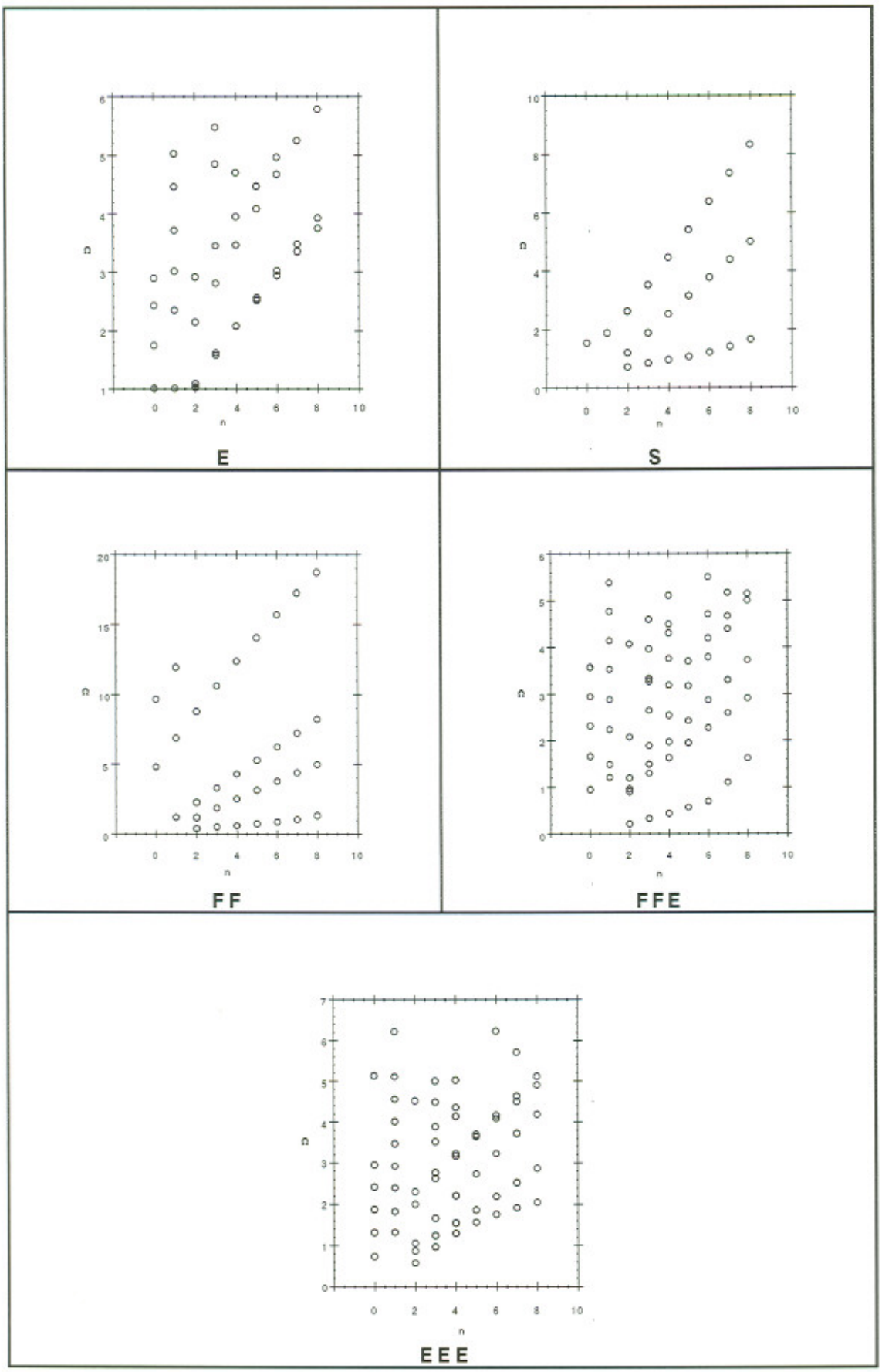

Figure 3: Eigenfrequency spectra of the E -, S -, FF -, FFE - and EEE - models.

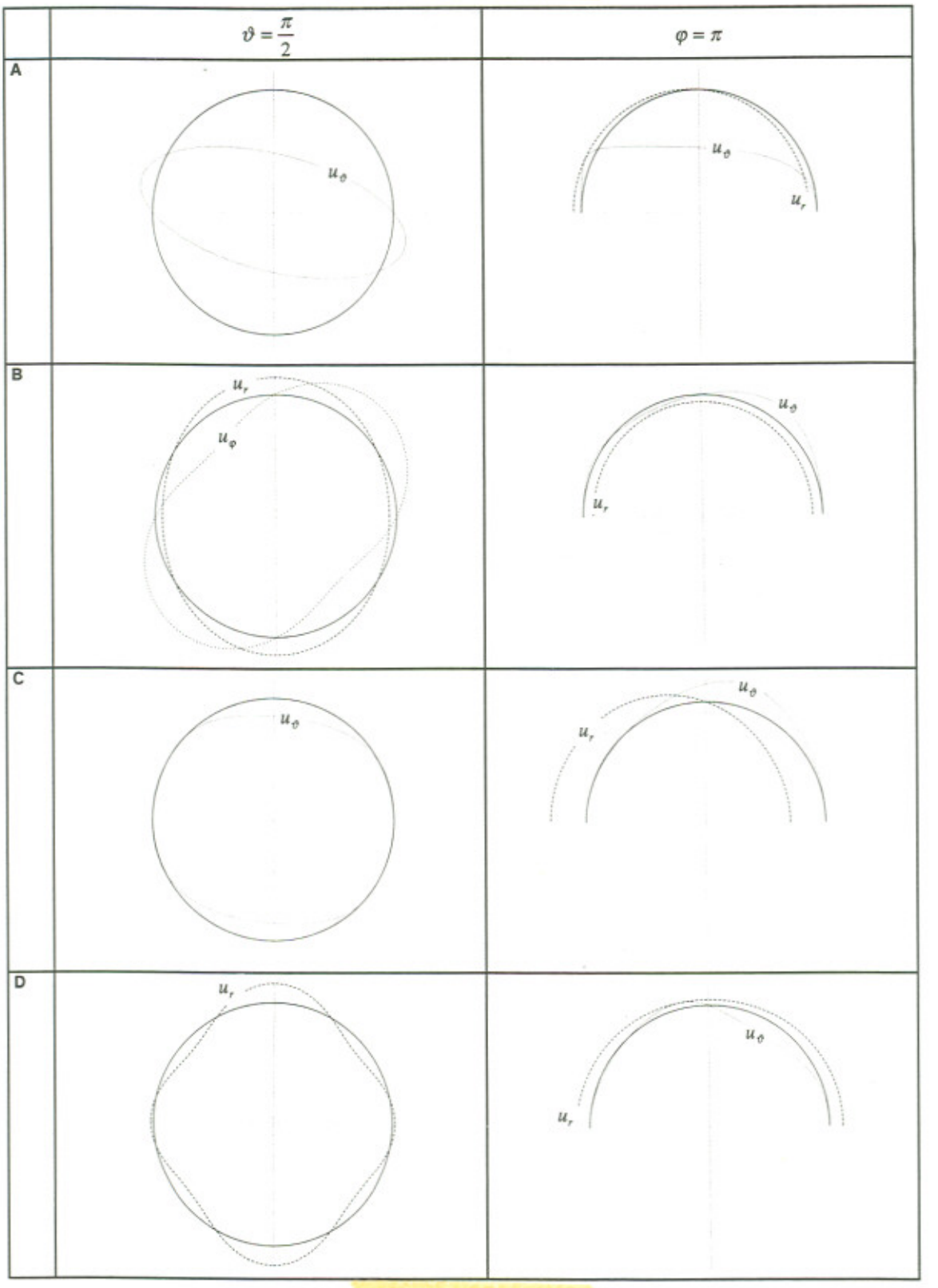

Figure 4: FFE - Model: Mode shapes for $(u_r, u_\varphi, u_\vartheta)$

(A: n=1 Ω_n=2.0247, B: n=2 Ω_n=0.8259, C: n=3 Ω_n=1.0793, D: n=4 Ω_n=1.3146)

Finally the results obtained are compared with the experimental ones presented in Ref. 3. Following the approximation adopted by Engin and Liu [4] and many other researchers about the cranial system geometry and its physical properties we used the present analysis to calculate the eigenfrequencies of the FF - and FFE - models. For the purpose of comparison the results obtained as well as the experimental ones are presented in Table 6 and graphically in Fig. 5.

We observe that:

$$\omega_{FFE}^{(k)} < \omega_{\text{exp.}}^{(k)} < \omega_{FF}^{(k)}, \quad k = 1,2,....,19$$

and also that the resonance frequencies are > 483 Hz. The analysis on the basis of the FFE - and FF - models predicts nineteen and six frequencies ≤ 3650 Hz, respectively, while the measured ones are only ten.

Table 6: Eigenfrequencies (Hz) of the human skull - brain system [3].

No.	Experimental Results [3] (mean values)	Standard Deviation [3]	Present Analysis (FF - model)	Present Analysis (FFE - model)	Mean Value of FF - and FFE - models
1	972	119	1423	483	953
2	1230	148	1843	797	1320
3	1532	159	2191	1121	1656
4	1785	169	2580	1435	2007
5	2076	217	3068	1518	2293
6	2287	203	3636	1544	2590
7	2568	308	4125	1889	3007
8	2899	389	4261	2035	3148
9	3253	381	4535	2371	3453
10	3590	377	5775	2386	4080
11	4101	543	6737	2544	4640
12	4793	596	6920	2640	4780
13	5304	660	7987	2826	5406
14	5766	807	8303	3085	5694
15	5841	419	8629	3146	5887
16	6336	539	9040	3333	6186
17	6656	429	11270	3534	7402
18	6883	176	11560	3559	7559
19	7165	.....	11580	3613	7596

It is remarkable to note that the estimation of the resonance frequencies of the human skull *in vivo* by the mean value of the corresponding ones to the FF - and FFE - models is in the range of the measurements presented by Håkansson et al., although we did not take into account the neck support as well as the viscous damping of the physical system.

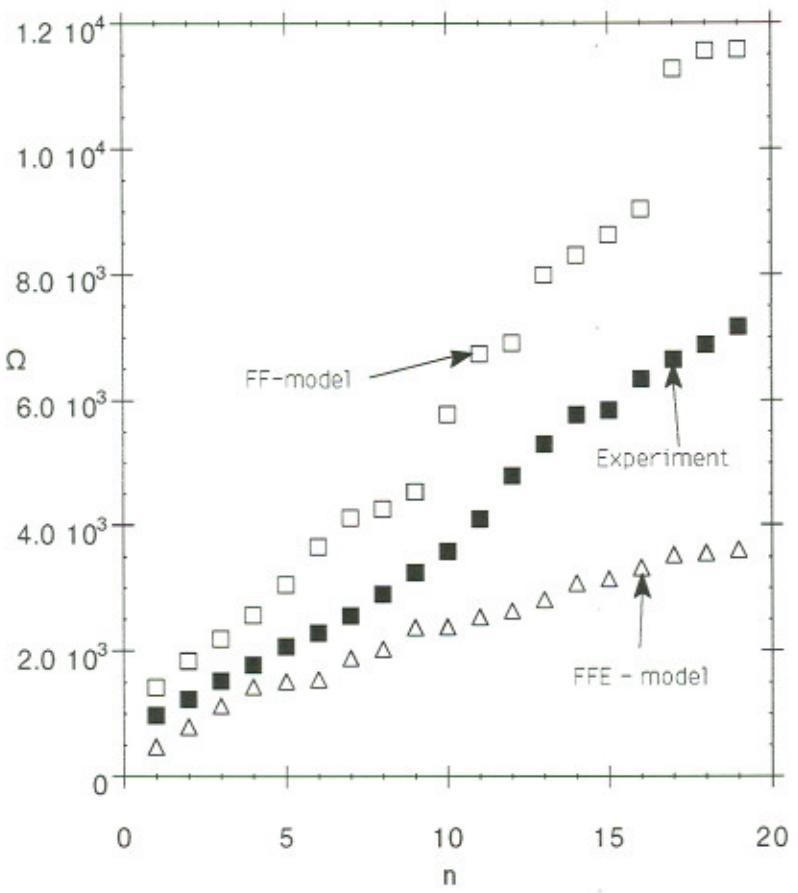

Figure 5: Comparison with Experiments (corresponds to Table 6)

5. CONCLUDING REMARKS

In this work we presented a mathematical analysis for the study of the dynamic characteristics of the human skull-brain system in the framework of the three - dimensional theory of elasticity. The geometry of the physical system considered has been modelled by the FFE - model where the outer hollow elastic sphere represents the skull, the inner elastic sphere corresponds to the brain and the space between them is supposed to be filled with the cerebrospinal fluid. The related FF -, EEE -, S -, and E - models are also discussed.

The proposed analysis was used to calculate the eigenfrequencies and the corresponding to them eigenmodes of the simulated physical system. The results obtained are in good agreement with the existing theoretical ones and further study is needed to simulate the real physical system. The reason of the disagreement between our results and the experimental ones are supposed to be due to the approximation of the materials entering the problem as well as the absence of the influence on the dynamic characteristics of the neck support. We observed that the presence of the inner sphere changes the natural frequencies spectra of a fluid - filled hollow elastic sphere. This change increases when the shell theory is extended to the three-dimensional theory of elasticity.

The dynamic analysis of the head-neck system as well as the simulation of the brain matter by a viscoelastic material are in preparation and will be presented in the future.

ACKNOWLEDGEMENT

The present work forms part of the project "New Systems for Early Medical Diagnosis and Biotechnological Applications" which is supported by the Greek General Secretariat for Research and Technology through the EU funded R&D Program EPET II.

REFERENCES

1. J.R. Guarino, Auscultatory percussion of the head, *British Medical Journal*, **284** 1075-1077 (1982).

2. T.B. Khalil and D.C. Viano, Experimental analysis of the vibrational characteristics of the human skull, *Journal of Sound and Vibration*, **63**(3) 351-376 (1979).

3. B. Håkansson, A. Brandt and P. Carlsson, Resonance frequencies of the human skull *in vivo*, *J. Acoust. Soc. Am.* **95**(3) 1474 - 1481 (1994)

4. A.E. Engin and Y.K. Liu, Axisymmetric response of a fluid filled spherical shell in free vibrations, *J. Biomechanics*, **3** 11-22 (1970)

5. S.H. Advani and R.P. Owings, Structural modelling of human head, *Journal of the Engineering Mechanics Division., American Society of Civil Engineers*, **101** 257-266 (1975).

6. O. Talhouri and F. Dimaggio, Dynamic response of a fluid-filled spheroidal shell - an improved model for studying head injury, *J. Biomechanics*, **8** 219-228 (1975).

7. J.C. Mirsa and S. Chakravarty, Dynamic response of a head - neck system to an impulsive load, *Mathematical Modelling*, **6** 83-96 (1985).

8. J.C. Guarino and D.F. Elger, Modal analysis of a fluid-filled elastic shell containing an elastic sphere, *Journal of Sound and Vibration*, **156**(3) 461-479 (1992).

9. T.C. Su, The effect of viscosity on the free oscillations of fluid filled spherical shell, *Journal of Sound and Vibration*, **74**(2) 205-220 (1981).

10. K.B. Sahay, R. Mehrotra, U. Sachdera and A.K. Bonerji, Elastomechanical Characterization of brain tissues, *J. Biomechanics*, **25** (3) 319-326 (1992).

11. M.R. Pamidi and S.H. Advani, Nonlinear constitutive relations for human brain tissue, *J. Biomech. Engng. Trans. ASME*, **100** 44-48 (1978).

12. A. Charalambopoulos, G. Dassios, D. I. Fotiadis, V. Kostopoulos, C. V. Massalas, On the Dynamic Characteristics of the Human Skull, *International Journal of Engineering Science*, Submitted (1996).

13. J.H. McElhaney, Mechanical properties of Cranial Bone, *J. Biomechanics*, **3** 495-511 (1970).

14. T.B. Khalil and R.P. Hubbard, Parametric Study Of Head Response by Finite Element Modelling, *J. Biomechanics*, **10** 119-132 (1977).

15. R. Hickling and M. L. Wenner, Mathematical model of a head subjected to an axisymmetric impact, *J. Biomechanics*, **6** 115-132 (1973).

APPENDIX A:

The spherical polar coordinates of the real part of the displacement field for the region 2 are:

$$u_{or}^{(2)}=\sum_{n=0}^{\infty}\sum_{m=-n}^{n}\sum_{l=1}^{2}\left\{\begin{array}{l}\alpha_{n,2}^{m,l}\dot{g}_n^l(k'_{p_2},r')\cos(m\varphi)P_n^m(\cos\vartheta)+\\ \gamma_{n,2}^{m,l}(n(n+1))\dfrac{g_n^l(k'_{s_2}r')}{k'_{s_2}r'}\cos(m\varphi)P_n^m(\cos\vartheta)\end{array}\right\}$$

$$u_{o\vartheta}^{(2)}=\sum_{n=0}^{\infty}\sum_{m=-n}^{n}\sum_{l=1}^{2}\left\{\begin{array}{l}\alpha_{n,2}^{m,l}\dfrac{g_n^l(\Omega r')}{\Omega r'}\cos(m\varphi)\dfrac{\partial}{\partial\vartheta}P_n^m(\cos\vartheta)\\ -\beta_{n,2}^{m,l}g_n^l(k'_{s_2}r')\dfrac{m\sin(m\varphi)}{\sin\vartheta}P_n^m(\cos\vartheta)\\ +\gamma_{n,2}^{m,l}(\dot{g}_n^l(k'_{s_2}r')+\dfrac{g_n^l(k'_{s_2}r')}{k'_{s_2}r'})\cos(m\varphi)\dfrac{\partial}{\partial\vartheta}P_n^m(\cos\vartheta)\end{array}\right\}$$

$$u_{o\varphi}^{(2)}=\sum_{n=0}^{\infty}\sum_{m=-n}^{n}\sum_{l=1}^{2}\left\{\begin{array}{l}-\alpha_{n,2}^{m,l}\dfrac{g_n^l(\Omega r')}{\Omega r'}\dfrac{m\sin(m\varphi)}{\sin\vartheta}P_n^m(\cos\vartheta)\\ -\beta_{n,2}^{m,l}g_n^l(k'_{s_2}r')\cos(m\varphi)\dfrac{\partial}{\partial\vartheta}P_n^m(\cos\vartheta)\\ -\gamma_{n,2}^{m,l}(\dot{g}_n^l(k'_{s_2}r')+\dfrac{g_n^l(k'_{s_2}r')}{k'_{s_2}r'})\dfrac{m\sin(m\varphi)}{\sin\vartheta}P_n^m(\cos\vartheta)\end{array}\right\}.$$

The expressions $\boldsymbol{T}'_i\boldsymbol{L}_n^{m,l}(\hat{\boldsymbol{r}}')$, $\boldsymbol{T}'_i\boldsymbol{M}_n^{m,l}(\hat{\boldsymbol{r}}')$ and $\boldsymbol{T}'_i\boldsymbol{N}_n^{m,l}(\hat{\boldsymbol{r}}')$ are:

$$\boldsymbol{T}'_i\boldsymbol{L}_n^{m,l}(\hat{r})=-\left[\frac{4\mu'_i}{r'}\dot{g}_n^l(\Omega r')+2\mu'_i\Omega(1-\frac{n(n+1)}{\Omega^2r'^2})g_n^l(\Omega r')+\lambda'_i\Omega g_n^l(\Omega r')\right]\boldsymbol{P}_n^m(\hat{r})$$

$$+2\mu'_i\sqrt{n(n+1)}\left[\frac{\dot{g}_n^l(\Omega r')}{r'}-\frac{g_n^l(\Omega r')}{\Omega r'^2}\right]\boldsymbol{B}_n^m(\hat{r})$$

$$\boldsymbol{T}'_i\boldsymbol{M}_n^{m,l}(\hat{r})=\mu'_i\sqrt{n(n+1)}\left[k'_{s_i}\dot{g}_n^l(k'_{s_i}r')-\frac{1}{r'}g_n^l(k'_{s_i}r')\right]\boldsymbol{C}_n^m(\hat{r})$$

$$\boldsymbol{T}'_i\boldsymbol{N}_n^{m,l}(\hat{r})=2\mu'_i n(n+1)\left[\frac{\dot{g}_n^l(k'_{s_i}r')}{r'}-\frac{g_n^l(k'_{s_i}r')}{k'_{s_i}r'^2}\right]\boldsymbol{P}_n^m(\hat{r})$$

$$+\mu'_i\sqrt{n(n+1)}\left[-2\frac{\dot{g}_n^l(k'_{s_i}r')}{r'}-k'_{s_i}g_n^l(k'_{s_i}r')+2\frac{n(n+1)-1}{k'_{s_i}r'^2}g_n^l(k'_{s_i}r')\right]\boldsymbol{B}_n^m(\hat{r})$$

APPENDIX B: $\boldsymbol{Dx} = \boldsymbol{0}$, $\boldsymbol{D} = [d_{i,j}]$

Case 1: Elastic Sphere (E - model)

$$\begin{bmatrix} A_n^1(r_2) & 0 & D_n^1(r_2) \\ 0 & \Gamma_n^1(r_2) & 0 \\ B_n^1(r_2) & 0 & E_n^1(r_2) \end{bmatrix} \begin{bmatrix} \alpha_n^m \\ \beta_n^m \\ \gamma_n^m \end{bmatrix} = \boldsymbol{0}$$

Case 2: Fluid - Filled Elastic Sphere (FF - model)

$$\begin{bmatrix} A_n^1(r_2) & A_n^2(r'_2) & 0 & 0 & D_n^1(r'_2) & D_n^2(r'_2) & 0 \\ B_n^1(r_2) & B_n^2(r'_2) & 0 & 0 & E_n^1(r'_2) & E_n^2(r'_2) & 0 \\ 0 & 0 & \Gamma_n^1(r'_2) & \Gamma_n^2(r'_2) & 0 & 0 & 0 \\ A_n^1(r'_0) & A_n^2(r'_0) & 0 & 0 & D_n^1(r'_0) & D_n^2(r'_0) & d_{4,7} \\ B_n^1(r'_0) & B_n^2(r'_0) & 0 & 0 & E_n^1(r'_0) & E_n^2(r'_0) & 0 \\ 0 & 0 & \Gamma_n^1(r'_0) & \Gamma_n^2(r'_0) & 0 & 0 & 0 \\ d_{7,1} & d_{7,2} & 0 & 0 & d_{7,5} & d_{7,6} & d_{7,7} \end{bmatrix} \begin{bmatrix} \alpha_n^{m,1} \\ \alpha_n^{m,2} \\ \beta_n^{m,1} \\ \beta_n^{m,2} \\ \gamma_n^{m,1} \\ \gamma_n^{m,2} \\ c_{nm} \end{bmatrix} = \boldsymbol{0}$$

where

$$d_{4,7} = -i\Omega \frac{\rho'_f}{c'^2_s} g_n^1(k'_f r'_0),\ d_{7,1} = \dot{g}_n^1(\Omega r'_0),\ d_{7,2} = \dot{g}_n^2(\Omega r'_0),\ d_{7,5} = n(n+1)\frac{g_n^1(k'_s r'_0)}{k'_s r'_0}$$

$$d_{7,6} = n(n+1)\frac{g_n^2(k'_s r'_0)}{k'_s r'_0},\ d_{7,7} = \frac{i}{c'_f}\dot{g}_n^1(k'_f r'_0)$$

Case 3: Fluid - Filled Elastic Sphere Containing an Elastic Sphere (FFE - model)

In this case the vector $\boldsymbol{x}$ and the non - zero elements of the matrix $\boldsymbol{D}$ are

$$\boldsymbol{x} = \left[\alpha_{n,2}^{m,1} \quad \alpha_{n,2}^{m,2} \quad \beta_{n,2}^{m,1} \quad \beta_{n,2}^{m,2} \quad \gamma_{n,2}^{m,1} \quad \gamma_{n,2}^{m,2} \quad \alpha_{n,0}^{m} \quad \beta_{n,0}^{m} \quad \gamma_{n,0}^{m} \quad c_{nm} \quad d_{nm}\right]^T$$

$$d_{1,1} = A_{n,2}^{1}(r'_2),\ d_{1,2} = A_{n,2}^{2}(r'_2),\ d_{1,5} = D_{n,2}^{1}(r'_2),\ d_{1,6} = D_{n,2}^{2}(r'_2),$$
$$d_{2,1} = E_{n,2}^{1}(r'_2),\ d_{2,2} = E_{n,2}^{2}(r'_2),\ d_{2,5} = E_{n,2}^{1}(r'_2),\ d_{2,6} = E_{n,2}^{2}(r'_2)$$

$$d_{3,3} = \Gamma_{n,2}^{1}(r'_2),\ d_{3,4} = \Gamma_{n,2}^{2}(r'_2)$$

$$d_{4,1} = A_{n,2}^{1}(r'_1),\ d_{4,2} = A_{n,2}^{2}(r'_1),\ d_{4,5} = D_{n,2}^{1}(r'_1),\ d_{4,6} = D_{n,2}^{2}(r'_1)$$

$$d_{4,10} = \Omega\rho'_f \frac{1}{c'^2_{s_2}} g_n^1(k'_f r'_1),\ d_{4,11} = \Omega\rho'_f \frac{1}{c'^2_{s_2}} g_n^2(k'_f r'_1)$$

$$d_{5,1} = B_{n,2}^{1}(r'_1),\ d_{5,2} = B_{n,2}^{2}(r'_1),\ d_{5,5} = E_{n,2}^{1}(r'_1),\ d_{5,6} = E_{n,2}^{2}(r'_1)$$

$$d_{6,3} = \Gamma_{n,2}^{1}(r'_1),\ d_{6,4} = \Gamma_{n,2}^{2}(r'_1)$$

$$d_{7,1} = \dot{g}_n^1(\Omega r'_1),\ d_{7,2} = \dot{g}_n^2(\Omega r'_1),\ d_{7,5} = n(n+1)\frac{g_n^1(k'_{s_2} r'_1)}{k'_{s_2} r'_1}$$

$$d_{7,6} = n(n+1)\frac{g_n^2(k'_{s_2} r'_1)}{k'_{s_2} r'_1},\ d_{7,10} = -\frac{1}{c'_f}\dot{g}_n^1(k'_f r'_1),\ d_{7,11} = -\frac{1}{c'_f}\dot{g}_n^2(k'_f r'_1)$$

$$d_{8,7} = A_{n,0}^{1}(r'_0),\ d_{8,9} = D_{n,0}^{1}(r'_0),\ d_{8,10} = \Omega\rho'_f \frac{1}{c'^2_{s_2}} g_n^1(k'_f r'_0),\ d_{8,11} = \Omega\rho'_f \frac{1}{c'^2_{s_2}} g_n^2(k'_f r'_0)$$

$$d_{9,7} = B_{n,0}^{1}(r'_0),\ d_{9,9} = E_{n,0}^{1}(r'_0)$$

$$d_{10,8} = \Gamma_{n,0}^{1}(r'_0)$$

$$d_{11,7} = \dot{g}(k'_{p_0} r'_0),\ d_{11,9} = n(n+1)\frac{g_n^1(k'_{s_0} r'_0)}{k'_{s_0} r'_0},\ d_{11,10} = -\frac{1}{c'_f}\dot{g}_n^1(k'_f r'_0)$$

$$d_{11,10} = -\frac{1}{c'_f}\dot{g}_n^1(k'_f r'_0)$$

Case 4: Three Elastic Spheres (EEE - model)

In this case the vector $\boldsymbol{x}$ and the non - zero elements of the matrix $\boldsymbol{D}$ are

$$\boldsymbol{x}=\left[\alpha_{n,2}^{m,1}\quad \alpha_{n,2}^{m,2}\quad \beta_{n,2}^{m,1}\quad \beta_{n,2}^{m,2}\quad \gamma_{n,2}^{m,1}\quad \gamma_{n,2}^{m,2}\quad \alpha_{n,1}^{m,1}\quad \alpha_{n,1}^{m,2}\quad \beta_{n,1}^{m,1}\quad \beta_{n,1}^{m,2}\quad \gamma_{n,1}^{m,1}\quad \gamma_{n,1}^{m,2}\quad \alpha_{n,0}^{m}\quad \beta_{n,0}^{m}\quad \gamma_{n,0}^{m}\right]^{T}$$

$$d_{1,1}=A_{n,2}^{1}(r'_2),\ d_{1,2}=A_{n,2}^{2}(r'_2),\ d_{1,5}=D_{n,2}^{1}(r'_2),\ d_{1,6}=D_{n,2}^{2}(r'_2)$$

$$d_{2,1}=E_{n,2}^{1}(r'_2),\ d_{2,3}=\Gamma_{n,2}^{2}(r'_2),\ d_{2,4}=\Gamma_{n,2}^{1}(r'_2)$$

$$d_{3,1}=B_{n,2}^{1}(r'_2),\ d_{3,2}=B_{n,2}^{2}(r'_2),\ d_{3,5}=E_{n,2}^{1}(r'_2),\ d_{3,6}=E_{n,2}^{2}(r'_2)$$

$$d_{4,1}=\dot{g}_n^{1}(\Omega r'_1),\ d_{4,2}=\dot{g}_n^{2}(\Omega r'_1)$$

$$d_{4,5}=n(n+1)g_n^{1}(\Omega\sqrt{(2+\frac{\lambda'_2}{\mu'_2})}r'_1)\frac{1}{\Omega\sqrt{(2+\frac{\lambda'_2}{\mu'_2})}r'_1}$$

$$d_{4,6}=n(n+1)g_n^{2}(\Omega\sqrt{(2+\frac{\lambda'_2}{\mu'_2})}r'_1)\frac{1}{\Omega\sqrt{(2+\frac{\lambda'_2}{\mu'_2})}r'_1}$$

$$d_{4,7}=-g_n^{1}(\xi_{p,21}\Omega r'_1),\ d_{4,8}=-g_n^{2}(\xi_{p,21}\Omega r'_1)$$

$$d_{4,11}=-n(n+1)g_n^{1}(\xi_{p,21}\Omega\sqrt{(2+\frac{\lambda'_2}{\mu'_2})}r'_1)\frac{1}{\xi_{p,21}\Omega\sqrt{(2+\frac{\lambda'_2}{\mu'_2})}r'_1}$$

$$d_{4,12}=-n(n+1)g_n^{2}(\xi_{p,21}\Omega\sqrt{(2+\frac{\lambda'_2}{\mu'_2})}r'_1)\frac{1}{\xi_{p,21}\Omega\sqrt{(2+\frac{\lambda'_2}{\mu'_2})}r'_1}$$

$$d_{5,3}=g_n^{1}(\Omega\sqrt{(2+\frac{\lambda'_2}{\mu'_2})}r'_1),\ d_{5,4}=g_n^{2}(\Omega\sqrt{(2+\frac{\lambda'_2}{\mu'_2})}r'_1),\ d_{5,9}=-g_n^{1}(\xi_{p,21}\Omega\sqrt{(2+\frac{\lambda'_2}{\mu'_2})}r'_1)$$

$$d_{5,10}=-g_n^{2}(\xi_{p,21}\Omega\sqrt{(2+\frac{\lambda'_2}{\mu'_2})}r'_1)$$

$$d_{6,1}=\dot{g}_n^{1}(\Omega r'_1)\frac{1}{\Omega r'_1},\ d_{6,2}=\dot{g}_n^{2}(\Omega r'_1)\frac{1}{\Omega r'_1}$$

$$d_{6,5}=\dot{g}_n^{1}(\Omega\sqrt{2+\frac{\lambda'_2}{\mu'_2}}r'_1)+\frac{g_n^{1}(\Omega\sqrt{2+\frac{\lambda'_2}{\mu'_2}}r'_1)}{\Omega\sqrt{2+\frac{\lambda'_2}{\mu'_2}}r'_1}$$

$$d_{6,5} = \dot{g}_n^2(\Omega\sqrt{2+\frac{\lambda'_2}{\mu'_2}}r'_1) + \frac{g_n^2(\Omega\sqrt{2+\frac{\lambda'_2}{\mu'_2}}r'_1)}{\Omega\sqrt{2+\frac{\lambda'_2}{\mu'_2}}r'_1}$$

$$d_{6,7} = -\frac{g_n^1(\xi_{p,21}\Omega r'_1)}{\xi_{p,21}\Omega r'_1},\ d_{6,8} = -\frac{g_n^2(\xi_{p,21}\Omega r'_1)}{\xi_{p,21}\Omega r'_1}$$

$$d_{6,11} = -\left[\dot{g}_n^1(\xi_{p,21}\Omega\sqrt{2+\frac{\lambda'_1}{\mu'_1}}r'_1) + \frac{g_n^1(\xi_{p,21}\Omega\sqrt{2+\frac{\lambda'_1}{\mu'_1}}r'_1)}{\xi_{p,21}\Omega\sqrt{2+\frac{\lambda'_1}{\mu'_1}}r'_1}\right]$$

$$d_{6,12} = -\left[\dot{g}_n^2(\xi_{p,21}\Omega\sqrt{2+\frac{\lambda'_1}{\mu'_1}}r'_1) + \frac{g_n^2(\xi_{p,21}\Omega\sqrt{2+\frac{\lambda'_1}{\mu'_1}}r'_1)}{\xi_{p,21}\Omega\sqrt{2+\frac{\lambda'_1}{\mu'_1}}r'_1}\right]$$

$$d_{7,1} = A_{n,2}^1(r'_1),\ d_{7,2} = A_{n,2}^2(r'_1),\ d_{7,5} = D_{n,2}^1(r'_1),\ d_{7,6} = D_{n,2}^2(r'_1), d_{7,7} = -A_{n,1}^1(r'_1)$$

$$d_{7,8} = -A_{n,1}^2(r'_1), d_{7,11} = -D_{n,1}^1(r'_1), d_{7,12} = -D_{n,1}^2(r'_1)$$

$$d_{8,3} = \Gamma_{n,2}^1(r'_1),\ d_{8,4} = \Gamma_{n,2}^2(r'_1), d_{8,9} = \Gamma_{n,1}^1(r'_1), d_{8,10} = \Gamma_{n,1}^2(r'_1)$$

$$d_{9,1} = B_{n,2}^1(r'_1), d_{9,2} = B_{n,2}^2(r'_1),\ d_{9,5} = E_{n,2}^1(r'_1), d_{9,6} = E_{n,2}^2(r'_1)$$

$$d_{9,7} = -B_{n,1}^1(r'_1), d_{9,8} = -B_{n,1}^2(r'_1), d_{9,11} = -E_{n,1}^1(r'_1), d_{9,12} = -E_{n,1}^2(r'_1)$$

$$d_{10,7} = \dot{g}_n^1(\xi_{p,21}\Omega r'_0),\ d_{10,8} = \dot{g}_n^2(\xi_{p,21}\Omega r'_0)$$

$$d_{10,11} = n(n+1)g_n^1(\xi_{p,21}\Omega\sqrt{2+\frac{\lambda'_1}{\mu'_1}}r'_0)\frac{1}{\xi_{p,21}\Omega\sqrt{2+\frac{\lambda'_1}{\mu'_1}}r'_0}$$

$$d_{10,12} = n(n+1)g_n^2(\xi_{p,21}\Omega\sqrt{2+\frac{\lambda'_1}{\mu'_1}}r'_0)\frac{1}{\xi_{p,21}\Omega\sqrt{2+\frac{\lambda'_1}{\mu'_1}}r'_0}$$

$$d_{10,13} = -\dot{g}_n^1(\xi_{p,20}\Omega r'_0)$$

$$d_{10,15} = -n(n+1)\frac{g_n^1(\xi_{p,20}\Omega\sqrt{2+\frac{\lambda'_0}{\mu'_0}}r'_0)}{\xi_{p,20}\Omega\sqrt{2+\frac{\lambda'_0}{\mu'_0}}r'_0}$$

$$d_{11,9} = g_n^1(\xi_{p,21}\Omega\sqrt{2+\frac{\lambda'_1}{\mu'_1}}r'_0),\ d_{11,10} = g_n^2(\xi_{p,21}\Omega\sqrt{2+\frac{\lambda'_1}{\mu'_1}}r'_0)$$

$$d_{11,14} = -g_n^1(\xi_{p,20}\Omega\sqrt{2+\frac{\lambda'_0}{\mu'_0}}r'_0)$$

$$d_{12,7} = g_n^1(\xi_{p,21}\Omega r'_0)\frac{1}{\xi_{p,21}\Omega r'_0},\ d_{12,8} = g_n^2(\xi_{p,21}\Omega r'_0)\frac{1}{\xi_{p,21}\Omega r'_0}$$

$$d_{12,11} = \dot{g}_n^1(\xi_{p,21}\Omega\sqrt{2+\frac{\lambda'_1}{\mu'_1}}r'_0)+\frac{g_n^1(\xi_{p,21}\Omega\sqrt{2+\frac{\lambda'_1}{\mu'_1}}r'_0)}{\xi_{p,21}\Omega\sqrt{2+\frac{\lambda'_1}{\mu'_1}}r'_0}$$

$$d_{12,12} = \dot{g}_n^2(\xi_{p,21}\Omega\sqrt{2+\frac{\lambda'_1}{\mu'_1}}r'_0)+\frac{g_n^2(\xi_{p,21}\Omega\sqrt{2+\frac{\lambda'_1}{\mu'_1}}r'_0)}{\xi_{p,21}\Omega\sqrt{2+\frac{\lambda'_1}{\mu'_1}}r'_0}$$

$$d_{12,13} = -g_n^1(\xi_{p,20}\Omega r'_0)\frac{1}{\xi_{p,20}\Omega r'_0}$$

$$d_{12,15} = -\left[\dot{g}_n^1(\xi_{p,20}\Omega\sqrt{2+\frac{\lambda'_0}{\mu'_0}}r'_0)+\frac{g_n^1(\xi_{p,20}\Omega\sqrt{2+\frac{\lambda'_0}{\mu'_0}}r'_0)}{\xi_{p,20}\Omega\sqrt{2+\frac{\lambda'_0}{\mu'_0}}r'_0}\right]$$

$$d_{13,7} = A_{n,1}^1(r'_0),\ d_{13,8} = A_{n,1}^2(r'_0),\ d_{13,11} = D_{n,1}^1(r'_0),\ d_{13,12} = D_{n,1}^2(r'_0)$$

$$d_{13,13} = -A_{n,0}^1(r'_0),\ d_{13,15} = -D_{n,0}^1(r'_0)$$

$$d_{14,9} = \Gamma_{n,1}^1(r'_0),\ d_{14,10} = \Gamma_{n,1}^2(r'_0),\ d_{14,14} = -\Gamma_{n,0}^2(r'_0)$$

$$d_{15,7} = B_{n,1}^1(r'_0),\ d_{15,8} = B_{n,1}^2(r'_0),\ d_{15,11} = E_{n,1}^1(r'_0)$$

$$d_{15,12} = E_{n,1}^2(r'_0),\ d_{15,13} = -B_{n,0}^1(r'_0),\ d_{15,15} = -E_{n,0}^1(r'_0)$$

where $\xi_{p,2i} = \frac{c_{p_2}}{c_{p_i}}$.